

Pushing the Limits of the Eigenstate Thermalization Hypothesis towards Mesoscopic Quantum Systems

R. Steinigeweg,^{1,*} A. Khodja,² H. Niemeyer,² C. Gogolin,³ and J. Gemmer^{2,†}

¹*Institute for Theoretical Physics, Technical University Braunschweig, D-38106 Braunschweig, Germany*

²*Department of Physics, University of Osnabrück, D-49069 Osnabrück, Germany*

³*Dahlem Center for Complex Quantum Systems, Freie Universität Berlin, D-14195 Berlin, Germany*

(Dated: November 3, 2018)

In the ongoing discussion on thermalization in closed quantum many-body systems, the eigenstate thermalization hypothesis (ETH) has recently been proposed as a universal concept which attracted considerable attention. So far this concept is, as the name states, hypothetical. The majority of attempts to overcome this hypothetical character is based on exact diagonalization which implies for, e.g., spin systems a limitation to roughly 15 spins. In this Letter we present an approach which pushes this limit up to system sizes of roughly 35 spins, thereby going significantly beyond what is possible with exact diagonalization. A concrete application to a Heisenberg spin-ladder which yields conclusive results is demonstrated.

PACS numbers: 03.65.Yz, 75.10.Jm, 05.45.Pq

Introduction. Due to experiments in ultracold atomic gases [1–5], the question of thermalization in closed quantum systems has experienced an upsurge of interest in recent years, and the eigenstate thermalization hypothesis (ETH) has become a cornerstone of the theoretical understanding of thermalizing quantum many-body systems. The ETH roughly postulates the following [6–8]: Eigenstates of a Hamiltonian H in certain energy regions exhibit properties similar or equal to the properties of a statistical ensemble, e.g., canonical or microcanonical corresponding to that energy region. The properties in this context can be manifold: expectation values of certain observables, entropies or purities of subsystems of an interacting system, etc. Regardless of its significance in the debate on thermalization [8, 9], it is a challenging task to “check” numerically whether or not the ETH applies to a specific system and property. If this is done in a straightforward manner, it requires the diagonalization of the Hamiltonian [10–14]. Due to the exponential scaling of the Hilbert space dimension, this is only feasible for rather limited system sizes. Considering, e.g., spin systems without any symmetries, numerical diagonalization using state-of-the-art computers and routines is feasible up to about 15 spins.

While numerical diagonalization of quantum systems is costly, the approximation of exponentials of (functions of) the Hamiltonian H applied to a pure state vector, i.e., expressions of the form

$$|\psi(\tau)\rangle \equiv e^{\tau H} |\psi\rangle \quad (1)$$

(τ being some complex number), has lately seen substantial progress. Methods in this direction include or are related to time-dependent density matrix renormalization group (tDMRG) [15–17], Lanczos [18] or Chebyshev [19] integrator codes. tDMRG allows to reach system sizes of the order of 100 or 200 lattice sites [20], not only in spin

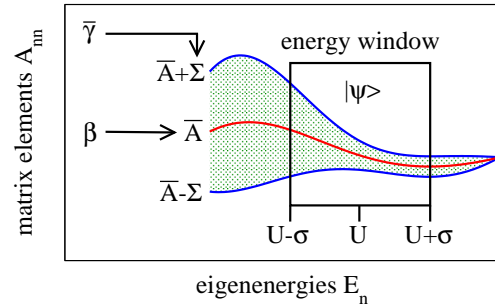


FIG. 1. (color online) Sketch of the question: In the energy eigenbasis the diagonal elements $A_{nn} = \langle n|A|n\rangle$ of a given observable A are in general not a smooth function of energy, but distributed around their average \bar{A} in a region of width 2Σ ; the ETH breaks down when Σ is significantly larger than zero. We present a scheme that accurately approximates \bar{A} and Σ by two other quantities β and $\bar{\gamma}$. The latter can be calculated on the basis of random state vectors $|\psi\rangle$ that live in energy windows $[U - \sigma, U + \sigma]$, once operator exponentials can be applied to pure state vectors in a numerical way.

systems [21]. It is however somewhat limited regarding system geometries and initial states: systems must be more or less linear and initial states usually need to be in some sense close to the ground state. Lanczos and Chebyshev are at present limited to systems comprising about 35 spins [18, 22, 23], however, pure initial states may be chosen arbitrarily and the only requirement on the Hamiltonian is a sparse structure when represented w.r.t. some reasonable, practically accessible basis [24]. This wider range of applicability makes especially the Chebyshev integrator a good candidate for future applications of the methods introduced here.

In the remainder of this Letter we present a scheme that allows for the computation of ETH-related data on the basis of numerical codes performing the application

of matrix exponentials in the sense of Eq. (1). Apart from the computation of matrix exponentials, the scheme only requires the “equilibration” of the addressed observable in the sense discussed in Refs. [25–28] on a time scale within the reach of the matrix-exponentiation code.

The scheme. Before explaining the scheme in detail, we specify more precisely what it eventually provides. Given a non-degenerate Hamiltonian H and an observable A of a system with Hilbert space dimension d . Then, in the context of the ETH, the following two quantities are of interest:

$$\bar{A} \equiv \sum_{n=1}^d p_n \langle n|A|n \rangle, \quad \Sigma^2 \equiv \sum_{n=1}^d p_n \langle n|A|n \rangle^2 - \bar{A}^2 \quad (2)$$

with $H|n\rangle = E_n|n\rangle$, $p_n \propto e^{-(E_n-U)^2/2\sigma^2}$, and $\sum_n p_n = 1$, i.e., $|n\rangle$ are eigenstates of the Hamiltonian and $(p_n)_d$ is a Gaussian probability vector with standard deviation σ . Thus, $\bar{A} = \bar{A}(U, \sigma)$ is a weighted average of the expectation values of A in the eigenstates of H that is most sensitive to an energy region of width σ around U , and $\Sigma^2 = \Sigma^2(U, \sigma)$ is a weighted variance corresponding to this energy region.

The relation to the ETH is the following: if the ETH applies, the expectation values are supposed to be a smooth function of energy, i.e., the variance Σ^2 should become small for sufficiently small σ . In this sense, Σ^2 encodes information about the ETH. The scheme we are going to present in the following allows for a feasible computation of both, Σ^2 and \bar{A} . The smaller σ is, the more costly this calculation will be. However, we will present a concrete example in order to demonstrate the power of our approach.

The computational scheme we present relies on random state vectors. The fact that few random states suffice to obtain “non-random” information on the ETH is closely related to the concept of “typicality” [24, 26, 29–34]. It has been shown that state vectors drawn at random according to the distribution which is invariant under all unitary transformations (Haar measure) feature very similar expectation values for a given observable with high probability [30, 35]. Concretely, using the Hilbert space average method [35], one finds that the “Hilbert space average” (HA), i.e., the average of the expectation values for an observable A w.r.t. to the above distribution and the corresponding “Hilbert space variance” (HV) are given by

$$\text{HA}(\langle \psi|A|\psi \rangle) = \frac{\text{Tr}(A)}{d}, \quad (3)$$

$$\text{HV}(\langle \psi|A|\psi \rangle) = \frac{1}{d+1} \left[\frac{\text{Tr}(A^2)}{d} - \text{HA}^2 \right]. \quad (4)$$

Equipped with these results, we now describe the scheme.

First step. We start by defining an operator C ,

$$C \equiv e^{-\frac{(H-U)^2}{4\sigma^2}}, \quad (5)$$

which we will later use as an “energy filter”. (Similar “filters” have been used previously, e.g., in Refs. [36–38]). We are interested in computing $\text{Tr}(C^2)$ since this will be needed as a normalization constant below. To this end we consider the random variable

$$\alpha \equiv d \langle \psi|C^2|\psi \rangle, \quad (6)$$

where $|\psi\rangle$ is a random state vector drawn according to the above distribution. If we are able to apply matrix exponentials to random pure state vectors, we are able to compute random realizations of α . Using Eq. (3), we immediately find

$$\text{HA}(\alpha) = \overline{\text{Tr}(C^2)} = \sum_{n=1}^d e^{-\frac{(E_n-U)^2}{2\sigma^2}}. \quad (7)$$

The average of α is the quantity we are interested in. If the distribution of α was broad, estimating its HA would be costly since it would require computing many realizations of α . But from Eq. (4) we may directly read off an upper bound on the variance of α :

$$\text{HV}(\alpha) < \frac{d}{d+1} \text{Tr}(C^4) \leq \sum_{n=1}^d e^{-\frac{(E_n-U)^2}{\sigma^2}} \quad (8)$$

We cannot directly compute the sums in Eqs. (7) and (8); however, we can reasonably guess their scaling with the density of states $n(E)$. If $n(E)$ is a sufficiently smooth function to be linearized on a scale of σ around U , then the sums yield approximately

$$\text{Tr}(C^2) \approx \sqrt{2\pi}\sigma n(U), \quad \text{Tr}(C^4) \approx \sqrt{\pi}\sigma n(U). \quad (9)$$

Let us abbreviate $\sigma n(U) \equiv d_{\text{eff}}$. The meaning of d_{eff} is that of an effective dimension. The number of states in the respective energy window is roughly d_{eff} . If the size of a quantum system is increased while σ is kept fixed, d_{eff} can be expected to become very large rather quickly. Thus, w.r.t. d_{eff} , the average of α and an upper bound to its variance read in the limit of large d

$$\text{HA}(\alpha) \approx \sqrt{2\pi} d_{\text{eff}}, \quad \text{HV}(\alpha) \lesssim \sqrt{\pi} d_{\text{eff}}. \quad (10)$$

Since the standard deviation scales with the square root of the variance, the distribution of α with mean $\text{HA}(\alpha) \propto d_{\text{eff}}$ has the width $\sqrt{\text{HV}(\alpha)} \propto \sqrt{d_{\text{eff}}}$. Because the mean of α is the quantity of interest, calculating one α from one random $|\psi\rangle$ amounts to the determination of the wanted quantity with a relative error on the order of $1/\sqrt{d_{\text{eff}}}$. Thus, if d_{eff} is large enough, calculating only very few realizations of α will suffice.

Second step. Next we define

$$\rho \equiv \frac{C^2}{\text{Tr}(C^2)}, \quad (11)$$

which is a positive operator with trace one, i.e., a quantum state, and consider its application to a pure state

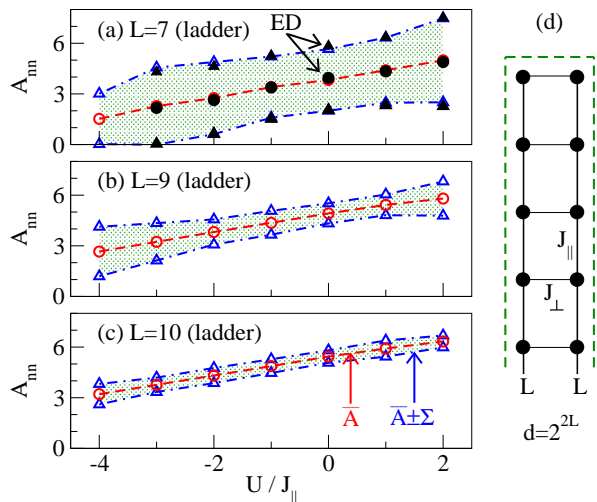


FIG. 2. (color online) The “cloud” of matrix elements A_{nm} for (a) $L = 7$, (b) 9, and (c) 10, obtained numerically using the scheme and 10 random state vectors. Panel (a) further provides a comparison with exact-diagonalization (filled symbols), clearly indicating negligibly small deviations of our scheme already for $L = 7$. Panel (d) is a sketch of the ladder model (solid lines) and its reduction to a chain (dashed lines).

vector. We note that $\langle m|\rho|n\rangle = p_n \delta_{nm}$. In order to determine \bar{A} , we also define and consider

$$\beta \equiv d \langle \psi | \sqrt{\rho} A \sqrt{\rho} | \psi \rangle. \quad (12)$$

Using again Eqs. (3) and (4), and following the same line of reasoning as in the context of α , we readily find the average of β and an upper bound to its variance:

$$\text{HA}(\beta) = \text{Tr}(\rho A) = \bar{A}, \quad (13)$$

$$\text{HV}(\beta) < \frac{d}{d+1} \text{Tr}(\rho A \rho A) \quad (14)$$

Again the average of β is the quantity of interest, and its computation is feasible if $\text{HV}(\beta)$ is small. (Note that it is not $\text{HV}(\beta)$ from which the desired Σ is eventually calculated.) To upper bound the variance, we write:

$$\text{Tr}(\rho A \rho A) = \sum_{m,n} p_n \langle n|A|m\rangle p_m \langle m|A|n\rangle \quad (15)$$

From Eqs. (5), (9) [l.h.s.], (11) we find $p_n \leq 1/d_{\text{eff}}$, which implies:

$$\text{Tr}(\rho A \rho A) \leq \sum_{m,n} \frac{p_n \langle n|A|m\rangle \langle m|A|n\rangle}{d_{\text{eff}}} = \frac{\text{Tr}(\rho A^2)}{d_{\text{eff}}} \quad (16)$$

If A is taken to be traceless (w.l.o.g.), for large d the variance $\text{HV}(\beta)$ is essentially upper-bounded by a term that scales as the, say, largest squared eigenvalue of A divided by the effective dimension d_{eff} . The largest eigenvalue of physical observables scales at most polynomially with system size, the effective dimension typically increases

exponentially. Hence, by calculating only a few β , it should be possible to determine \bar{A} within a relative error $\propto 1/\sqrt{d_{\text{eff}}}$.

Third step. Next, aiming at Σ , we consider

$$\gamma(t) \equiv d \langle \psi | \sqrt{\rho} A(t) A \sqrt{\rho} | \psi \rangle, \quad (17)$$

where $A(t)$ refers to the Heisenberg picture. Again, given the possibility to apply matrix exponentials to arbitrary state vectors, $\gamma(t)$ can be computed for random state vectors $|\psi\rangle$. To proceed, one has to require that $\gamma(t)$ not only relaxes with time to some value and then does not deviate much from that value [25–28], but, moreover, this must happen on time scales which are “short” compared to the time scales over which $\gamma(t)$ can be approximated numerically. If this applies, a time average from the relaxation time t_1 to the largest time t_2 reachable with the given resource will very accurately approximate the average over infinite time. Whether or not the above condition holds has to be guessed (or postulated), as well as the precise choice of t_1 and t_2 . However, the graph of $\gamma(t)$ itself may give good evidence and suggest a reasonable choice for t_1, t_2 . If the above holds, we find

$$\bar{\gamma} = \frac{1}{t_2 - t_1} \int_{t_1}^{t_2} dt \gamma(t) \approx d \langle \psi | \sqrt{\rho} A_D A \sqrt{\rho} | \psi \rangle \quad (18)$$

with A_D being the diagonal part of A in the energy eigenbasis. The random variable $\bar{\gamma}$ is very similar to β , c.f. Eq. (12). Going through precisely the same arguments that follow Eq. (12), one finds (still for large d)

$$\text{HA}(\bar{\gamma}) \approx \text{Tr}(\rho A_D A) = \Sigma^2 + \bar{A}^2, \quad (19)$$

$$\text{HV}(\bar{\gamma}) \lesssim \frac{1}{d_{\text{eff}}} \text{Tr}(\rho A_D A^2 A_D). \quad (20)$$

As before, if the largest eigenvalue of A does not scale exponentially with system size, Σ may be determined from a few realizations of $\bar{\gamma}$ within an error $\propto 1/\sqrt{d_{\text{eff}}}$.

Application. Eventually, we illustrate the introduced scheme using a Heisenberg spin ladder of length L without periodic boundary conditions as an example. The Hamiltonian $H = J_{\parallel} H_{\parallel} + J_{\perp} H_{\perp}$ reads ($\hbar = 1$)

$$H_{\parallel} = \sum_{r=1}^{L-1} \sum_{i=1}^2 S_{r,i}^x S_{r+1,i}^x + S_{r,i}^y S_{r+1,i}^y + \Delta S_{r,i}^z S_{r+1,i}^z, \\ H_{\perp} = \sum_{r=1}^L S_{r,1}^x S_{r,2}^x + S_{r,1}^y S_{r,2}^y + \Delta S_{r,1}^z S_{r,2}^z, \quad (21)$$

where $S_r^{x,y,z}$ are spin-1/2 operators at site (r, i) , $J_{\parallel} > 0$ is the antiferromagnetic exchange coupling constant along the legs, and $J_{\perp} = 0.2 J_{\parallel}$ is a small rung interaction. The exchange anisotropy $\Delta = 0.6$ is chosen to realize several non-thermalizing properties of the legs alone [13]. The Hamiltonian preserves the total magnetization S_{total}^z and is non-degenerate except for a two-fold degeneracy due to “particle-hole symmetry” [13, 39]. We choose the largest

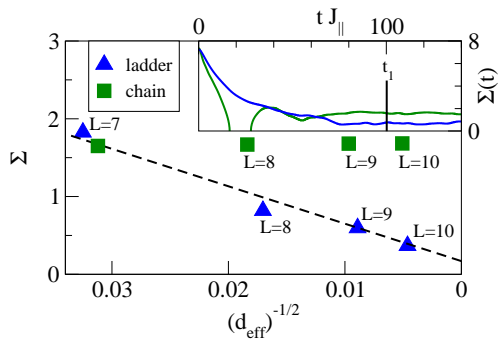


FIG. 3. (color online) The “cloud” width Σ as a function of the effective-dimension power $(d_{\text{eff}})^{-1/2}$ at energy $U = 0$ for the non-integrable ladder in Fig. 2 and an integrable chain. As a guide to the eye, the line indicates a function $\propto (d_{\text{eff}})^{-1/2}$, where the offset at $(d_{\text{eff}})^{-1/2} \rightarrow 0$ ($L \rightarrow \infty$) is given by $\sigma d\bar{A}/dU \approx 0.17$ as the product of the chosen energy-window width σ and the “cloud” slope $d\bar{A}/dU$, see the discussion in the text for details. The inset shows the underlying graph of $\Sigma(t)$ for $L = 10$, with the relaxation time t_1 indicated.

“half-filling” subspace $S_{\text{total}}^z = 0$. This non-integrable ladder reduces to an integrable chain if $J_{\perp} = J_{\parallel}$ and only the first rung is kept in H_{\perp} , see Fig. 2 (d).

We study the magnetization difference $\delta M = \sum_{r=1}^L S_{r,1}^z - S_{r,2}^z$ of the two legs. Due to the “particle-hole symmetry”, any energy eigenstate must necessarily yield $\langle n | \delta M | n \rangle = 0$ and describes the magnetization as being equally distributed between the two legs. Hence, one could say that the ETH is fulfilled w.r.t. the observable δM . This, however, does not mean that in every single measurement the magnetization on each of the two legs is $\pm L/2$, which would be true only if $\langle n | \delta M^2 | n \rangle = 0$. But the latter is not trivially fulfilled since δM^2 shares “particle-hole” symmetry other than δM . Therefore, δM^2 may possibly vary from eigenstate to eigenstate.

A recent publication [40] reported that $\langle \psi(t) | \delta M | \psi(t) \rangle$ and $\langle \psi(t) | \delta M^2 | \psi(t) \rangle$ relax to some values, almost regardless of the initial state (restricted to a window of energy). While this is not very surprising for δM , it hints towards the validity of the ETH w.r.t. δM^2 . Since the behavior described in Ref. [40] becomes pronounced only above $L = 8$, numerically checking the ETH is a highly non-trivial task. We show that with our proposed scheme it is however possible to convincingly verify numerically the validity of the ETH w.r.t. the observable $A = \delta M^2$.

We begin with state vectors $|\psi(0)\rangle = \sum_i c_i |i\rangle$, where the set of state vectors $|i\rangle$ is the Ising basis in the convenient spin- \uparrow/\downarrow representation, in the subspace $S_{\text{total}}^z = 0$. The coefficients c_i are obtained by generating independent Gaussian random numbers with mean zero and variance one for the real and imaginary part. In order to compute realizations of α from Eq. (6), the “energy-filter” operator C in Eq. (5) is approximated by a fourth order Runge-Kutta integrator [41], iterating in imaginary

time with a discrete time step δt until the chosen energy window is reached. For all calculations we choose $\sigma = 0.37$, which is small compared to the width of the spectrum of H . Using the same imaginary-time iteration, the mean of β in Eq. (12) can also be approximated. Similarly, a real-time iteration [41] provides the technical foundation for the calculation of $\gamma(t)$ in Eq. (17), starting from two different energy-filtered initial state vectors, first $C|\psi(0)\rangle$ and second $\delta M^2 C|\psi(0)\rangle$. The choice of t_1 and t_2 in Eq. (18) is made manually by reading off times where $\gamma(t)$ does not show any kind of dynamics apart from minor oscillations (see the inset of Fig. 3).

Figure 2 (a) compares the scheme to results from exact diagonalization for $L = 7$. Apparently, the agreement is remarkably good for a rather small system, supporting that the mean of β and $\bar{\gamma}$ indeed yield good approximations of the exact average \bar{A} and variance Σ . Figure 2 (b) shows the results for the “cloud” center $\bar{A} \approx \beta$ and the “cloud” width $\Sigma \approx \sqrt{\bar{\gamma} - \beta^2}$ but now for $L = 9$ and 10. While Σ very clearly decreases with L , $\bar{A} \propto L$ due δM being extensive [40], but the slope of \bar{A} as a function of energy stays the same.

The question of how the “cloud” width Σ scales with the system size can be answered by plotting it against the effective dimension d_{eff} in Eq. (9) for some energy interval in Fig. 2. For convenience, Fig. 3 shows Σ vs. the effective-dimension power $(d_{\text{eff}})^{-1/2}$. Clearly, Fig. 3 supports the scaling $\Sigma \propto (d_{\text{eff}})^{-1/2}$. Such a scaling is expected for random Hamiltonians [14] and is consistent with the non-integrability of our model. Even though there is a remaining offset at $(d_{\text{eff}})^{-1/2} \rightarrow 0$ ($L \rightarrow \infty$), this offset does *not* indicate the breakdown of the ETH for our observable and model. In fact, the offset is a minimum “cloud” width $\sigma d\bar{A}/dU \approx 0.17$ given by the product of the chosen energy-window width σ and the “cloud” slope $d\bar{A}/dU$. To illustrate how the breakdown of the ETH can be detected by our approach, Fig. 3 shows also results on the integrable chain ($J_{\perp} = J_{\parallel}$ and a single rung in H_{\perp}), where Σ does not depend on system size.

Conclusion. In this paper we presented an innovative scheme for deciding whether or not the ETH is valid in a given closed many-body quantum system of finite but very large Hilbert space dimension. Using the framework of typicality, we showed that both, average and variance of the diagonal matrix elements of a given observable in the energy eigenbasis can be calculated from a single or few pure state vectors, if the application of operator exponentials is available in a numerical way. We demonstrated the latter for a prototypical spin model by using a Runge-Kutta iterator. While Runge-Kutta will allow for more than 20 spins in cases with several symmetries [42], sophisticated algorithms like Chebyshev integrators, when used with our scheme, will enable almost exact studies of the ETH in systems of up to 35 spins [22, 23] and provide further insight into thermalization in large closed quantum many-body systems.

We gratefully acknowledge financial support by the *Deutsche Forschungsgemeinschaft* and the *Stiftung des Deutschen Volkes*.

* r.steinigeweg@tu-bs.de

† jgemmer@uos.de

- [1] S. Trotzky *et al.*, *Science* **319**, 295 (2007).
 [2] S. Hofferberth *et al.*, *Nature* **449**, 324 (2007).
 [3] I. Bloch, J. Dalibard, and W. Zwerger, *Rev. Mod. Phys.* **80**, 885 (2008).
 [4] M. Cheneau *et al.*, *Nature* **481**, 484 (2012).
 [5] T. Langen *et al.*, *Nature Phys.* **9**, 640 (2013).
 [6] J. M. Deutsch, *Phys. Rev. A* **43**, 2046 (1991).
 [7] M. Srednicki, *Phys. Rev. E* **50**, 888 (1994).
 [8] M. Rigol, V. Dunjko, and M. Olshanii, *Nature* **452**, 854 (2008).
 [9] M. Rigol and M. Srednicki, *Phys. Rev. Lett.* **108**, 110601 (2012).
 [10] M. Rigol, *Phys. Rev. Lett.* **103**, 100403 (2009).
 [11] L. F. Santos and M. Rigol, *Phys. Rev. E* **82**, 031130 (2010).
 [12] M. Rigol and L. F. Santos, *Phys. Rev. A* **82**, 011604(R) (2010).
 [13] R. Steinigeweg, J. Herbrich, and P. Prelovšek, *Phys. Rev. E* **87**, 012118 (2013).
 [14] W. Beugeling, R. Moessner, and M. Haque, preprint, arXiv:1308.2862 (2013).
 [15] A. J. Daley *et al.*, *J. Stat. Mech.* P04005 (2004).
 [16] S. R. White and A. E. Feiguin, *Phys. Rev. Lett.* **93**, 076401 (2004).
 [17] G. Vidal, *Phys. Rev. Lett.* **93**, 040502 (2004).
 [18] For a recent review on Lanczos see: P. Prelovšek and J. Bonča, *Ground State and Finite Temperature Lanczos Methods in Strongly Correlated Systems*, Solid-State Sciences **176** (Springer, Berlin, 2013).
 [19] H. De Raedt and K. Michielsen, *Computational Methods for Simulating Quantum Computers in Handbook of Theoretical and Computational Nanotechnology* (American Scientific Publishers, Los Angeles, 2006).
 [20] C. Karrasch, J. H. Bardarson, and J. E. Moore, *Phys. Rev. Lett.* **108**, 227206 (2012).
 [21] G. Biroli, C. Kollath, and A. M. Läuchli, *Phys. Rev. Lett.* **105**, 250401 (2010).
 [22] F. Jin *et al.*, *J. Phys. Soc. Jpn.* **79**, 124005 (2010).
 [23] K. De Raedt *et al.*, *Comp. Phys. Comm.* **176**, 121 (2007).
 [24] T. A. Elsayed and B. V. Fine, *Phys. Rev. Lett.* **110**, 070404 (2013).
 [25] P. Reimann, *Phys. Rev. Lett.* **101**, 190403 (2008).
 [26] N. Linden, S. Popescu, A. J. Short, and A. Winter, *Phys. Rev. E* **79**, 061103 (2009).
 [27] A. J. Short and T. C. Farrelly, *New J. Phys.* **14**, 013063 (2012).
 [28] P. Reimann and M. Kastner, *New J. Phys.* **14**, 043020 (2012).
 [29] S. Goldstein, J. L. Lebowitz, R. Tumulka, and N. Zanghi, *Phys. Rev. Lett.* **96**, 050403 (2006).
 [30] S. Popescu, A. J. Short, and A. Winter, *Nature Phys.* **2**, 754 (2006).
 [31] P. Reimann, *Phys. Rev. Lett.* **99**, 160404 (2007).
 [32] C. Bartsch and J. Gemmer, *Phys. Rev. Lett.* **102**, 110403 (2009).
 [33] S. Sugiura and A. Shimizu, *Phys. Rev. Lett.* **108**, 240401 (2012).
 [34] S. Sugiura and A. Shimizu, *Phys. Rev. Lett.* **111**, 010401 (2013).
 [35] J. Gemmer, M. Michel, and G. Mahler, *Quantum Thermodynamics: Emergence of Thermodynamic Behavior within Composite Quantum Systems*, Lect. Notes Phys. **657**, 2nd edition (Springer, Berlin, 2009).
 [36] C. Presilla and U. Tambini, *Phys. Rev. E* **52**, 4495 (1995).
 [37] S. Garnerone and T. R. de Oliveira, *Phys. Rev. B* **87**, 214426 (2013).
 [38] S. Garnerone, *Phys. Rev. B* **88**, 165140 (2013).
 [39] M. Žnidarič, *Phys. Rev. Lett.* **110**, 070602 (2013).
 [40] H. Niemeyer, D. Schmitke, and J. Gemmer, *EPL (Eur. Phys. Lett.)* **101**, 10010 (2013); H. Niemeyer *et al.*, in preparation.
 [41] Generally, a fourth order Runge-Kutta scheme has the form $|\psi(t + \delta t)\rangle = |\psi(t)\rangle + \sum_i |v_i\rangle$, $|v_1\rangle = O\delta t|\psi(t)\rangle$, $|v_2\rangle = O\delta t/2|v_1\rangle$, $|v_3\rangle = O\delta t/3|v_2\rangle$, $|v_4\rangle = O\delta t/4|v_3\rangle$ with $O = -(H - U)^2$ for energy filtering and $O = -\nu H$ for time evolution, cf. Ref. [24].
 [42] R. Steinigeweg, J. Gemmer, and W. Brenig, preprint, arXiv:1312.5319 (2013), to appear in *Phys. Rev. Lett.*